COBEM 2023 27TH INTERNATIONAL CONGRESS OF MECHANICAL ENGENEERING

ABCM Brazilian Society of Mechanical Sciences and Engineering
27th ABCM International Congress of Mechanical Engineering
December 04-08, 2023, Florianópolis-SC, Brazil

COB-2023-0130
INFLUENCES OF THE DYNAMIC WIRE FEEDING OF FLUX-CORED WIRE WITH WC IN GTAW PROCESS APPLIED TO HARDFACING COATINGS

Ivan Olszanski Pigozzo
Kaue Correa Riffel
Regis Henrique Gonçalves e Silva
LABSOLDA - Welding and Mechatronics Institute, Universidade Federal de Santa Catarina, campus Trindade, Florianópolis-SC, Brazil.
ivan.pigozzo@posgrad.ufsc.br, kaue.riffel@posgrad.ufsc.br, *regis.silva@ufsc.br*

Abstract: *High-hardness materials with increased wear resistance associated with corrosion resistance are constantly demanded in the mining and oil & gas industries. Thus, flux-cored wires with tungsten carbide have been used for hard-facing applications aiming for greater wear resistance requirements. In the present paper, single bead welding experiments were carried out to evaluate the influences of advanced techniques of dynamic wire feeding in GTAW process (with wire longitudinal oscillation) over the weld bead morphology and mechanical properties. Moreover, the effect of the wire oscillation over the spread of the tungsten carbides within the molten zone was evaluated. A comparison between conventional wire feeding versus dynamic wire feeding was conducted. The wire oscillation frequency was varied in 0, 5, 10, and 15Hz. The filler metal used was the CORODUR OA-Br (MF 21/22 UM-60-CG) flux-cored wire with tungsten carbides, manufactured by Durum do Brasil, laid over an ASTM A36 steel substrate. The weld metal macrographs and carbide dispersion were based on optical microscopy (OM). Chemical composition was also verified using EDS analysis. Vickers micro hardness with 1kg load and dry sand ASTM G65 wear resistance tests were also conducted. The main results showed that the increase of the wire's frequency reduced the weld bead reinforcement and dilution. Furthermore, wider weld beads were achieved with dynamic wires feeding. Regarding the tungsten carbide particles dispersion, the dynamic wire feeding results in a better and more uniform dispersion when compared to conventional wire feeding, which resulted in a greater weld bead surface hardness and abrasion resistance.*

Keywords: *Dynamic wire feeding, Hardfacing, Tungsten Carbides, GTAW.*

1. INTRODUCTION

Hardfacing technologies to enhance wear and corrosion resistance is widely used in mining, construction, agricultures, mineral processing, and other industry machineries. Components surface degradations is associated to many wear mechanisms such as abrasion, impacts, heat and corrosion, reducing its service life and leading to downtime and increased productions costs (Garbade and Dhokey, 2021).

Fe-based, Ni-based and Co-based coatings are commonly used to improve the surface wear and corrosion resistances (Ortiz et al., 2017; Ahn, 2013). Recently, solid particles, e.g. WC, TiC, were added into hardfacing alloys in order to obtain metal ceramic composites (MMC – Metal Matrix Composites), which has high hardness, good wear resistance and wettability (Xiao et al., 2021).

However, the coating wear behavior is not only associated to the presence of carbides, but also to the microstructures and phases of the weld metal matrix, as well to the carbide particles amount and distribution uniformity among the weld beads. Because of the higher density of the WC carbides (in the order of 8-9.5 g/cm³), it tends to concentrate in the bottom of the of the weld beads during the solidification process, resulting in non-homogenous distribution among the coating (Fan et al., 2019). Wu et al. (2004) and Acker et al. (2004) had shown that the carbides particles dispersion homogeneity is associated to the number of particles on the metal matrix. The authors have studied the percentage of WC particles added to Ni-based alloys and evaluated mechanical properties such as hardness and abrasion resistance. Fernandez et al. (2015) have shown that the higher the amount (wt%) of WC particles the higher is the matrix phase hardness on Ni-based alloys. The same result was obtained by Xu et al. (2011) when WC/Ni coatings with different contents of WC particles were evaluated. Garcia et al. (2016) state that the increase of matrix hardness is associated to the secondary carbides formation during the cladding process and, by the fact the WC particles contributes to generate a refined eutectic structure of the Ni alloy.

To perform hardfacing coatings processes, thermal spray (oxi-acetylen), Laser cladding, plasma and thermal spraying are commonly used. Although coatings made by Laser processes show advantages such as low porosity and good metallurgical bonding (Yang et al., 2012), the energy conversion efficiency is low (10 to 25%) and the high cost of

equipment still limits it in large-scale industrial applications (Liu et al., 2006). In this context, welding processes such as PTA (Plasma Transfer Arc), GMAW (Gas Metal Arc Welding) and GTAW (Gas Tungsten Arc Welding), cost much less than Laser welding and, still, can provide hard and wear resistant coatings with good metallurgical bonding at the clad layer-substrate interface (Lin et al., 2013). Investigations over GTAW hardfacing coatings also had shown that the weld matrix hardness is directly affected by number and size of carbide phases dissolved and finely MC-type dispersed carbides precipitated (Wang et al., 2021). The same work also shown that the more carbide particles per unit volume, the greater is the wear resistance. Yuan et al. (2023) correlates the mean distance between carbide particles and distribution pattern to the wear resistance of Ni-WC coating made by GTAW process. The author results shown that the closer are the particles the better is the coating wear resistance.

Regarding the GTAW process, recent works focuses the investigation over the wire feeding technique, more specifically, on the dynamic wire feeding. According to Pigozzo et al. (2022), dynamic wire feeding is a technique in which the wire speed is not constant, and it can be pulsed, where the wire moves only toward the molten pool with varied speed; or oscillated, where the wire moves forward and backward, longitudinally, with defined amplitude and frequency. The wire oscillation direct inflicts on weld bead geometry. Higher oscillation frequencies promote narrower weld beads with higher reinforcements (Riffel et al., 2020; and Cunha et al., 2022). The wire oscillation also promotes a better spreading of precipitates and higher grain refinement when compared to conventional wire feeding (Riffel et al. 2020).

In this context, the present work aims to evaluate the influence of dynamic wire feeding in the carbide particles dispersion among the weld beads. Micro-hardness and abrasion resistance were considered to compare the dynamic feeding with conventional wire feeding in the GTAW process. The weld bead geometry was also considered. The term “dynamic wire feeding” used in this work is associated with the oscillated dynamic wire feeding.

2. MATERIALS AND METHODS

ASTM A36 low carbon steel plates with 3/8” (9.52mm) of thickness were used to lay weld beads of 1.6 mm flux-cored wire with tungsten carbides. The filler metal used was the commercial Fe-based alloy CORODUR OA-Br (DIN 8555 MF 21/22 - UM - 60 – CG), manufactured by Durum do Brasil. The resultant weld bead consists in a C-Fe-W-Co matrix with dispersed tungsten carbides. According to the manufactures, the deposit presents elevated hardness (65-70 HRC) and high abrasion resistance. The base metal and filler composition are shown in Table 1 and Table 2 respectively.

Table 1 - Chemical composition of ASTM A36 steel plates.

ASTM A36 plate composition									
	C	Mn	Si	S	P	Cu	Cr	Ni	Mo
%Wt	0.14	0.51	0.17	0.014	0.016	0.10	0.11	0.05	0.012

Table 2 - chemical composition of Durum CORODUR OR-Br fluxed-core wire.

CORODUR OABR wire composition												
	Fe	C	Co	W	Mn	P	S	Si	Mg	Ti	Nb	Mo
%Wt	Bal.	≤ 2.5	≤ 5.0	≤ 30	≤ 0.2	≤ 0.02	≤ 0.015	≤ 0.2	≤ 0.015	≤ 0.40	≤ 0.2	≤ 0.15

For shielding gas, pure argon (99.99 % level of purity) was used, and the tungsten electrode was an AWS WGLa-15 with 3.2 mm in diameter and 40° sharpening angle. In the present work, the wire was inserted in the arc / molten pool through its front region in cold wire configuration. The wire feeding angle was 45° in relation to the electrode axis (Figure 1).

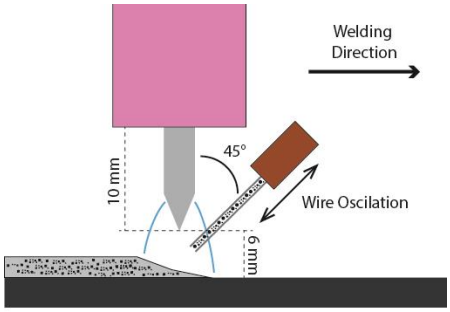

Figure 1 - Schematic diagram of wire feeding insertion and torch position.

The experiments were conducted in flat position by means of a three axes system for torch and specimen displacement. The power source was a multi-process IMC Digiplus A7 AC 450. For the wire longitudinal oscillation, it was used an oscillation module, developed by Labsolda - Welding and Mechatronics Institute, which allows the wire oscillation with frequencies adjustments up to 30 Hz and amplitude rage from 1 to 10 mm. The welding current (I), arc voltage (U_{arc}), electrode-to-wire voltage (U_{we}) and wire feed speed (WFS) were acquired by means of a data acquisition system at a sampling rate of 2 kHz. The data was later processed and analyzed in the Matlab software.

The experiments array consisted in two series: single beads over plate and clad samples. For the single bead series, the wire oscillation frequency was varied. It was used 0 Hz (no oscillation – conventional wire feeding), 5, 10 and 15 Hz (dynamic wire feeding). For the clad samples it was used 0 Hz (conventional wire feeding) and 10 Hz. The welding parameters are shown in Table 3.

Table 3 – Welding Parameters

Welding Parameter	Single bead	Overlay
Welding Current [A]	170	170
Arc Voltage(1) [V]	12.0	11.4
Power* [W]	2050	1976
Weaving amplitude [mm]	-	8.0
Weaving frequency [Hz]	-	1.0
Wire oscillation amplitude [mm]	8	8
Wire oscillation frequency [Hz]	0-5-10-15	0 - 10
Wire feed speed [m/min]	1	
Travel speed [mm/s]	2	
Arc Length [mm]	6	
Wire insertion angle	45°	
Cathode standoff distance [mm]	10	
Gas flow rate [l/min]	13	

(1)Average value acquired in all experiments (statistically equal).

Vickers microhardness tests were performed in the single bead samples using a Büehler Wilson VH1102 hardness tester. To evaluate the weld metal matrix, six indentations were performed at the central region of the weld bead under a load of 10N for 15s. For the weld bead surface micro-hardness, the top of the specimens was slightly sanded to flatten it. 10 indentations spaced with 0.4 mm were made per sample. The same load of 10N during 15s were used. Finally, carbide particles micro-hardness was measured with a load of 0.3N during 20s.

In addition to hardness testing, for the clad samples, ASTM G65 abrasion test was conducted with a 50 mesh dried sand under a load of 130N during 30 min. (6000 rotations in 200 rpm). The loss of weight was considered to evaluate de sample wear resistance. Figure 2 shows a schematic diagram of the test apparatus.

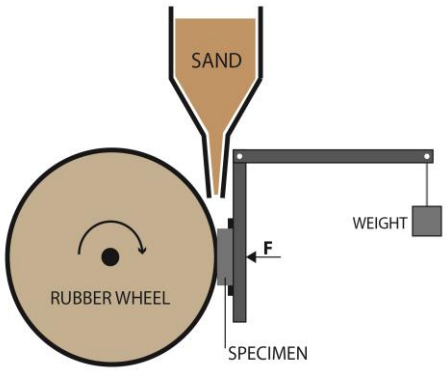

Figure 2 - ASTM G65 abrasion test schematic diagram.

The samples were cut, sanded (80, 220, 360, 600, and 1200 mesh), polished with Al_2O_3 and etched (Nital 10% solution). The weld bead photos were shot in a Zeiss Axiolab 5 optic microscope, and the geometry was measured by means of image processing software. The average values of reinforcement, width, max penetration, and geometric dilution were considered.

The carbides dispersion among the weld bead were evaluated by means of image post processing software Adobe Photoshop and Adobe Illustrator. The weld bead section was divided in four quadrants where the carbide particles were counted and measured.

Pearson correlation test and analysis of variation (ANOVA) probability test were used to evaluate the measured values.

3. RESULTS AND DISCUSSION

Figure 3 shows the single beads macrographs and the measured geometries are listed in Table 4. The increase of wire oscillation frequency resulted in a reduction of the weld bead reinforcement and higher width. For the 15 Hz bead, the reinforcement was 20.4 % less than 0 Hz (1.87 to 2.35 mm). For the 5 Hz and 10 Hz the reduction was 9.8 % (2.12 mm) and 10.6 % (2.10 mm) respectively when compared to no oscillation. Regarding the weld beads width, the 15 Hz experiment was 6.2 % wider than 0 Hz (9.87 and 9.29 mm respectively). For 5 Hz the increment was 2.5 % (9.52 mm), and for 10 Hz it was 5.6 % (9.81 mm).

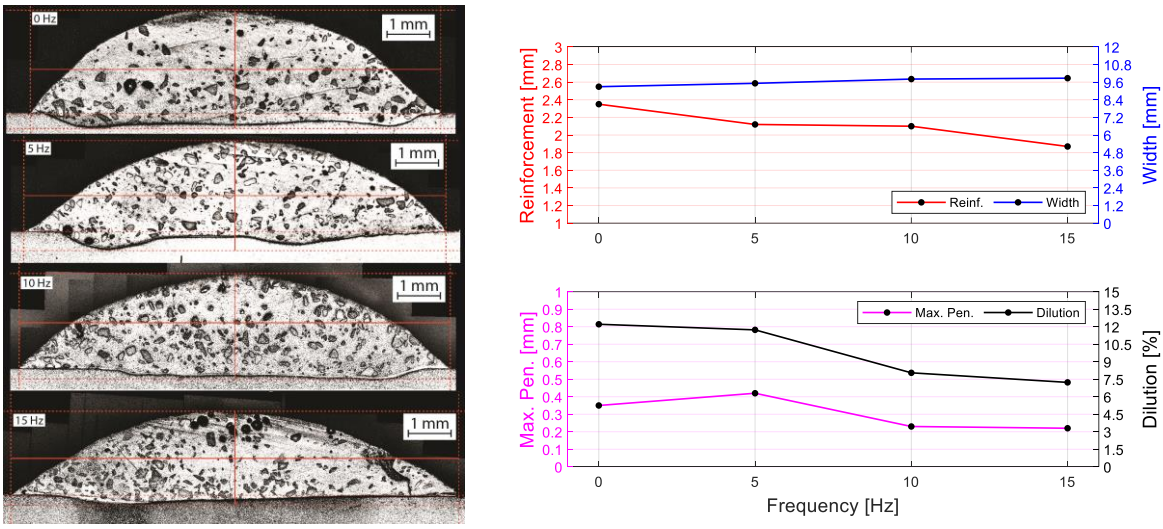

Figure 3 - (Left) Weld bead cross section macrograph's. (right) Weld bead geometry graphics.

The weld beads reinforcements and widths for the flux-cored wire varied on the opposite way compared to the results obtained by Riffel et al. (2020). The author suggests that the wire drags the melted pool during its forced backward movement due to surface tension action between wire' tip and molten pool. Even though, for the flux-cored wire, this behavior was on opposite way, and deeper investigations are necessary to explain it.

Still on the weld bead geometry, the maximum penetration was lower for 10 Hz (0.26 mm) and 15 Hz (0.22 mm) when compared to 0 Hz (0.35 mm). For 5 Hz it was higher (0.42 mm). Although the maximum penetration was higher for 5 Hz experiment, the weld bead dilution decreased, as well for the other experiments with dynamic wire feeding. For 0 Hz bead the dilution was 12.21 %. For 5, 10 and 15 Hz it decreased to 11.73, 8.05 and 7.20 % respectively. The results obtained for max penetration and dilution were in accordance with the results related by Riffel et al. (2020).

Table 4 – Weld bead measured geometry.

	Reinforcement (mm)	Max. Penetration (mm)	Width (mm)	Dilution (%)
0 Hz	2.35	0.35	9.29	12.21
5 Hz	2.12	0.42	9.52	11.73
10 Hz	2.10	0.26	9.81	8.05
15 Hz	1.87	0.22	9.87	7.20

Although no probability test was used to determine if there is a statistically significant difference between the measured geometries, Pearson Correlation Test was used to evaluate the strength of the linear relationship in between the oscillation frequency and the other variables. The Pearson Correlation Coefficient and p-value for each variable as listed in Table 5. The closer to 1 (or -1) is the correlation coefficient, the stronger is the relationship.

Table 5 – Correlation coefficients and probability values for weld bead geometry.

	Reinforcement	Width	Penetration	Dilution
r-coefficient[(1)]	-0.96	0.97	-0.79	-0.95
p-value	0.0389	0.026	0.211	0.048

[(1)]Correlation with the frequency variable

As it can be seen, there is a strong correlation in between the oscillation frequency with weld bead reinforcement, width, and dilution. For maximum penetration, it cannot be said that there is a linear correlation (p-value higher than 0.05) since the highest value was for the 5 Hz frequency.

Following with the analysis, the Vickers micro-hardness tests conducted over the weld metal matrix showed small variation in the values hardness's, which were 866.1, 841.1, 862.5 and 884.7 HV1 for 0, 5, 10 and 15 Hz respectively. The largest difference was in between 5 and 15 Hz (38.3 HV1 – 4.5%). Figure 4 shows the measured values for each indentation. By means of the analysis of variance (ANOVA), it is not possible to affirm that the average hardness's are different.

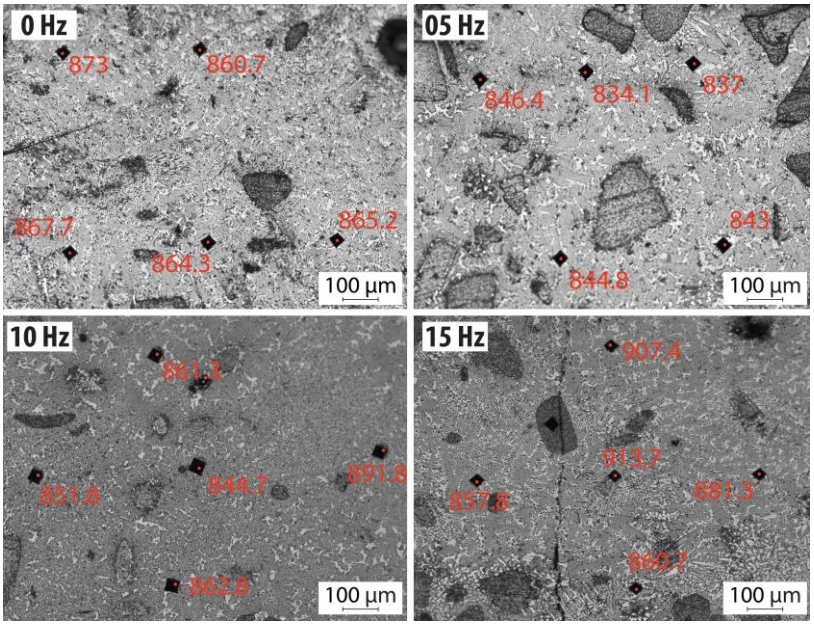

Figure 4 – Vickers micro-hardness indentations.

The measured values of the weld bead surface microhardness are listed on Table 6. As it can be seen, the dynamic wire feeding increased the weld bead surface hardness compared to the conventional wire feeding. For the 15 Hz sample, the surface hardness was 17.6 % greater than for the 0 Hz sample. Considering just the samples carried out with dynamic wire feeding, although the averages are different, it cannot be said that the surface microhardness has changed.

Table 6 – Weld bead surface measured micro-hardness.

Indentation	0 Hz	5 Hz	10 Hz	15 Hz
1	810.4	978.9	828.9	955.2
2	929.1	1042.0	1085.9	935.8
3	905.9	940.5	1012.3	1025.7
4	955.7	936.4	984.7	1090.9
5	1066.7	923.5	1049.2	913.3
6	914.7	993.4	1084.6	1152.4
7	798.9	1027.6	962.4	1171.6
8	836.6	1161.6	1049.0	1185.2
9	1006.3	1089.0	954.2	1124.2
Avrg.	902.3	1010.3	1001.2	1061.6
Std.	88.0	78.7	81.0	106.6
p-value(1) (ANOVA)	-	0.027	0.045	0.010

(1)probability-value comparing to the conventional wire feeding sample (0Hz)

Still on hardness testing, the dispersed carbide particles micro-hardness was also measured. The indentations were made over randomly selected particles at the surface region of the weld beads. The values varied from 1247.8 to 1596 HV0.3 with an average of 1460.5 HV0.3 (Table 7).

Table 7 – Carbides particles micro-hardness.

	0 Hz	**5 Hz**	**10 Hz**	**15 Hz**
Idt. 01 (HV0.3)	1530.6	1596.6	1506.0	1498.6
Idt. 02 (HV0.3)	1319.9	1247.8	1478.8	1546.8
Idt. 03 (HV0.3)	1523.4	1554.1	1375.6	1348.6
Average (HV0.3)	1458.0	1466.0	1453.5	1464.7

As it can be seen, the average values were similar in between the experiments, statistically, it can be said the average measured hardness are equal in the four conditions. Moreover, the carbide average hardness is approximately 62% greater the average surface hardness and almost 70% than the weld metal matrix for the 0Hz sample.

The increase of the surface hardness for the test carried out with dynamic wire feeding can be explained by the carbide particles dispersion pattern within the weld bead. The evaluation of the carbide's dispersion was done in the four quadrants of the sample cross-section area, as shown in Figure 5, and the percentage of the area in red (area covered by carbide particles) in relation to each quadrant area was considered. The values are listed in Table 8.

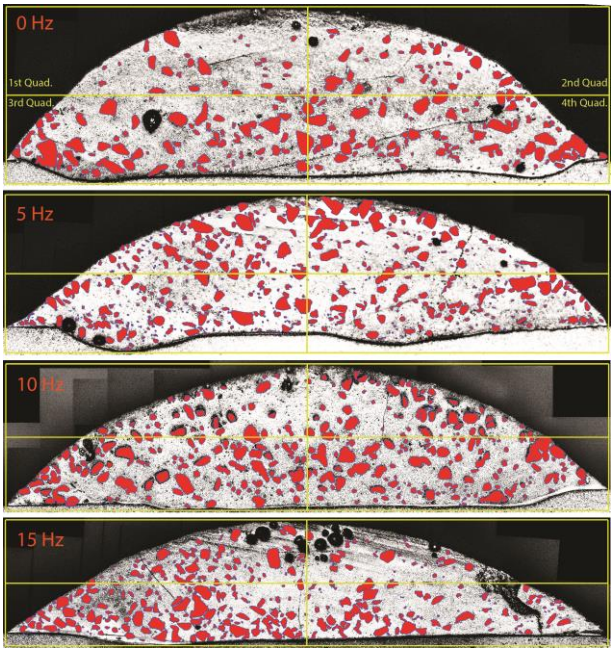

Figure 5 - Carbide particles covering areas.

Table 8 - Carbide particle covered area percentages by quadrants.

Specimen	**Quadrant**	**Carbide Area (%)**	**Specimen**	**Quadrant**	**Carbide Area (%)**
0 Hz (Conv.)	1st	12.0	**5 Hz**	1st	38.7
	2nd	19.9		2nd	47.7
	3rd	37.8		3rd	48.5
	4th	34.0		4th	42.5
	Avrg. / std	27.8 / 12.1		Avrg. / std	44.7 / 4.6
10 Hz	1st	20.1	**15 Hz**	1st	44.8
	2nd	26.2		2nd	21.8
	3rd	39.5		3rd	69.3
	4th	38.9		4th	43.5
	Avrg. / std	33.2 / 9.6		Avrg. / std	48.6 / 19.4

For the conventional wire feeding, the top quadrants (1st and 2nd) shown less carbides dispersed than the bottom quadrants (3rd and 4th). For the other experiments, the top quadrants also shown less area covered by the carbide particles,

but the percentages were higher. In this sample, the conventional wire feeding does not promote a forced agitation of the molten pool. Due to the higher density of carbide particles, it tends to accumulate at the bottom of the weld bead, as assessed (Fan et al., 2019).

The 5 Hz sample shown the biggest area covered by the particles in the top quadrants (38.7 and 47.7%). Furthermore, it presented the lowest standard deviation for the for quadrants (4.6%). The lower the standard deviation the more uniform is the carbide particles dispersion among the quadrants. The 15 Hz sample has the largest standard deviation values, but it also presented the most covered area (48.6 %). As it can be seen, the carbides particles are concentrated on the left quadrants, being the 3rd quadrant the one with the most covered area (69.3%). Although the standard deviation of the covered area compares the dispersion among the quadrants, the method suggested by Yuan et al. (2023), which consist to measure the distance between the carbides, is more appropriated to evaluate the homogeneity of carbide dispersion.

The better dispersion of the tungsten carbides for the 5, 10 and 15 Hz can be explained by the forced agitation promoted by the wire oscillation. Considering that the tungsten carbides, which are not dissociated into the matrix, are filled in solid state into the liquid metal, the more agitated is the molten pool, the better will be the particles spreading.

Besides the influence over the weld bead surface hardness, the carbide dispersion also reflected over the abrasion test results, which is strongly related to the hardness level of the sample.

The ASTM G65 abrasion test was conducted over the experiments with conventional wire feeding (0 Hz) and the dynamic wire feeding with 10 Hz. By the fact that the tungsten carbides particles hardness is much higher than the weld metal matrix, the more particles on the top quadrants, the higher is the wear resistance of the weld bead. The difference of mass loss in between the tests are shown in Table 9.

Table 9 – Abrasion test mass loss.

Specimen	Initial weight (g)	Final weight (g)	Mass loss (mg)
0 Hz	141.255	140.799	456 (ref.)
10 Hz	158.189	157.869	320 (- 29.8%)

As it can be seen, the test carried out with dynamic wire feeding (10 Hz) had and expressive reduction in the mass loss after the abrasive test, almost 30% less than the test carried out conventional wire feeding. In this case, the surface hardness and the carbide covered area of the top quadrants was 11% and 14% higher. According to Garcia et al. (2016), the wear resistance increases exponentially with the increase of WC concentration. Wang et al. (2021) measured the distribution density of WC particle on the weld bead surface and the higher the density, the greater is the wear resistance.

4. CONCLUSIONS

In the present paper, it was evaluated the influences of dynamic wire feeding of fluxed-cored wire over the weld bead geometries, hardness and abrasion resistance. Based on the results obtained, the following conclusions can be drawn:

- The dynamic wire feeding has strong influences over the weld bead geometry. For the flux-cored wire with WC particles, the higher the frequency the lower and wider is the weld bead reinforcement and width respectively. It also resulted in the decrease of the dilution;
- Although the weld metal matrix micro-hardness did no show significant variation among the samples, the dynamic wire feeding promoted higher hardness at the weld bead surfaces;
- The higher hardness at the surface can be associated to the carbide dispersion within the weld beads. For dynamic wire feeding, the dispersion was more uniform, and the top quadrants showed a larger covered area compared to the conventional wire feeding (0 Hz). Moreover, the most homogeneous dispersion of the carbides particles was at 5 Hz of wire oscillation frequency;
- The forced agitation of the molten pool promoted by the dynamic wire feeding resulted in a homogeneous carbide particle dispersion;
- The better carbide dispersion and higher surface hardness also reflected on the abrasion test. The sample carried out with dynamic wire feeding had 30% less mass loss than the conventional wire feeding, which promotes a greater longevity of the clad surfaces.

The results obtained are highly compelling for hardfacing coatings. Even though, more research and investigations are needed to better comprehend the technique for such applications. Future works could also compare the dynamic wire feeding with other welding processes and techniques already applied in global industries.

5. ACKNOWLEDGEMENTS

The authors acknowledge the Federal University of Santa Catarina and the Post-Graduate Program in Mechanical Engineering for providing the infrastructure, staff and technical support. Also, the author thanks PETROBRAS funding the development of this research, and to Durum do Brasil, for providing the investigated alloy.

6. REFERENCES

Van Acker, K., Vanhoyweghen, D., Persoons, R., Vangrunderbeek, J., 2005. “Influence of tungsten carbide particle size and distribution on the wear resistance of laser clad WC/Ni coatings”. *Wear*, 258, p. 194-202. Doi: 10.1016/j.wear.2004.09.041

Ahn, DG., 2013. “Hardfacing technologies for improvement of wear characteristics of hot working tools: A Review”. *International Journal of Precision Engineering and Manufacturing*, vol. 14, p. 1271–1283, 2013. Doi: 10.1007/s12541-013-0174-z

da Cunha, T.V., dos Santos, F.J. & Voigt, A.L., 2022. Study on the influence of operational conditions on weld bead morphology produced through TIG process with longitudinal wire oscillation. *J Braz. Soc. Mech. Sci. Eng*. 44, p. 292. Doi: 10.1007/s40430-022-03582-z

Fan, L., Dong, Y., Chen, H., Dong, L., Yin, Y., 2019. “Wear Properties of Plasma Transferred Arc Fe-based Coatings Reinforced by Spherical WC Particles”. *Journal of Wuhan University of Technology - Mater. Sci*. Ed. 34, p. 433–439. Doi: 10.1007/s11595-019-2070-6

Fernández, R., García, A., Cuetos, J.M., González, R., Noriega, A., Cadenas, M., 2015. “Effect of actual WC content on the reciprocating of a laser cladding NiCrBSi alloy reinforced with WC". *Wear*, 324-325, p. 80–89. Doi: doi.org/10.1016/j.wear.2014.12.021

Garbade, R. R., Dhokey, N.B., 2021. “Overview on Hardfacing Processes, Materials and Applications”. *IOP Conf. Series: Materials Science and Engineering, 1017*. Doi:10.1088/1757-899X/1017/1/012033

García, A., Fernández, M.R., Cuetos, J.M., González, R., Ortiz, A., Cadenas, M., 2016. “Study of the sliding wear and friction behavior of WC + NiCrBSi laser cladding coatings as a function of actual concentration of WC reinforcement particles in ball on disk test”. *Tribology.* Letters, 63, p. 41. Doi: 10.1007/s11249-016-0734-3

Lin, Y.C., Chen Y.C., 2013. “Reinforcements affect mechanical properties and wear behaviors of WC clad layer by gas tungsten arc welding”. *Materials and Design*, 45, p. 6–14. Doi: 10.1016/j.matdes.2012.08.055

Liu, YF., Xia, ZY., Han, JM., Zhang, GL., Yang SZ., 2006. “Microstructure and wear behavior of (Cr,Fe)7C3 reinforced composite coating produced by plasma transferred arc weld-surfacing process”. *Surface and Coatings Technology*, vol. 201, p. 863-867. Doi: 10.1016/j.surfcoat.2005.12.048

Ortiz, A. García, A., Cadenas, M., Fernández, M.R., Cuetos, J.M., 2017. “WC particles distribution model in the cross-section of laser cladded NiCrBSi +WC coatings, for different wt% WC”. *Surface and Coatings Technology*, 324, p. 298-306. Doi: 10.1016/j.surfcoat.2017.05.086

Riffel, K.C., Silva R.H.G., Haupt, W., Silva, L.E., 2020. “Effect of dynamic wire in the GTAW process: microstructure and corrosion resistance”. *Journal of Materials Processing Tech*. 285. Doi: 10.1016/j.jmatprotec.2020.116758

Wang, Y., Huang, Y., Yang, L., Sun, T., 2021. “Microstructure and property of tungsten carbide particulate reinforced wear seistant coating by TIG cladding”. *International Journal of Refractory Metals and Hard Materials*, vol. 100. Doi: 10.1016/j.ijrmhm.2021.105598

Xiao, Q., Sun, W.L., Yang, K.X., Xing, C.F., Chen, Z.H., Zhou, H.N., Lu, J., 2021. “Wear mechanisms and micro-evaluation on WC particles investigation of WC-Fe composite coatings fabricated by laser cladding”. *Surface & Coatings Technology*, 420. Doi: 10.1016/j.surfcoat.2021.127341

Xu, J.S., Zhang, X.C., Xuan, F.Z., Wang, Z.D., Tu, S.T., 2012. “Microstructure and sliding wear resistance of laser cladded WC/Ni composite coatings with different contents of WC particle”. *Journal of Materials Engineering and Performance*, 21, p. 194–1911. Doi: 10.1007/s11665-011-0109-8

Yang, MS., Liu, XB., Fan, JW., He, XM., Shi, SH., Fu, GY., Wang, MD., Chen, SF., 2012. "Microstructure and wear behaviors of laser clad NiCr/Cr3C2–WS2 high temperature self-lubricating wear-resistant composite coating". *Applied Surface Science*, vol. 258, p. 757-3762. Doi: 10.1016/j.apsusc.2011.12.021

Yuan, J., Huang, Y., Wang, L., Jia, C., Zhang, F., Yang, L., 2023. "Effect of the dissolution characteristic of tungsten carbide particles on microstructure and properties of Ni-WC/W2C reinforcement coating manufactured by TIG cladding". *International Journal of Refractory Metals and Hard Materials,* vol. 110. Doi: 10.1016/j.ijrmhm.2022.106047

7. RESPONSIBILITY NOTICE

The authors are the only responsible for the printed material included in this paper.